Cardiovascular Research (2015) **105**, 31–43
doi:10.1093/cvr/cvu218

# Nuclear pore rearrangements and nuclear trafficking in cardiomyocytes from rat and human failing hearts

**Mirna N. Chahine[1]*, Maxime Mioulane[1], Markus B. Sikkel[1], Peter O'Gara[1], Cristobal G. Dos Remedios[2], Grant N. Pierce[3], Alexander R. Lyon[1,4], Gábor Földes[1†], and Sian E. Harding[1†]**

[1]NHLI, Imperial College, London, UK; [2]Muscle Research Unit, Bosch Institute, The University of Sydney, Sydney, Australia; [3]Institute of Cardiovascular Sciences, St Boniface General Hospital Research Centre, University of Manitoba, Winnipeg, MB, Canada; and [4]NIHR Cardiovascular Biomedical Research Unit, Royal Brompton Hospital, London, UK

*Received 23 March 2014; revised 11 August 2014; accepted 14 August 2014; online publish-ahead-of-print 23 October 2014*

**Time for primary review: 14 days**

**Aims** During cardiac hypertrophy, cardiomyocytes (CMs) increase in the size and expression of cytoskeletal proteins while reactivating a foetal gene programme. The process is proposed to be dependent on increased nuclear export and, since nuclear pore trafficking has limited capacity, a linked decrease in import. Our objective was to investigate the role of nuclear import and export in control of hypertrophy in rat and human heart failure (HF).

**Methods and results** In myocardial tissue and isolated CMs from patients with dilated cardiomyopathy, nuclear size was increased; Nucleoporin p62, cytoplasmic RanBP1, and nuclear translocation of importins (α and β) were decreased while Exportin-1 was increased. CM from a rat HF model 16 weeks after myocardial infarction (MI) reproduced these nuclear changes. Nuclear import, determined by the rate of uptake of nuclear localization sequence (NLS)-tagged fluorescent substrate, was also decreased and this change was observed from 4 weeks after MI, before HF has developed. Treatment of isolated rat CMs with phenylephrine (PE) for 48 h produced similar cell and nuclear size increases, nuclear import and export protein rearrangement, and NLS substrate uptake decrease through p38 MAPK and HDAC-dependent pathways. The change in NLS substrate uptake occurred within 15 min of PE exposure. Inhibition of nuclear export with leptomycin B reversed established nuclear changes in PE-treated rat CMs and decreased NLS substrate uptake and cell/nuclear size in human CMs.

**Conclusions** Nuclear transport changes related to increased export and decreased import are an early event in hypertrophic development. Hypertrophy can be prevented, or even reversed, by targeting import/export, which may open new therapeutic opportunities.

**Keywords** Myocytes • Hypertrophy • Myocardial infarction • Signal transduction • Nuclear transport

## 1. Introduction

Heart failure (HF) remains a major cause of death worldwide.[1] (Refer to *Table 1* for all list of acronyms in the manuscript.) It is frequently preceded by cardiac hypertrophy defined as an adaptive process evolving from a physiological compensatory to a pathological maladaptive stage.[1,2] Pathological cardiac hypertrophy and HF are characterized not only by increases in cell size but also by the augmentation of cardiac gene expression including the reactivation of the foetal gene programme, as well as by cytoskeletal reorganization, leading eventually to decrease in cardiac function.[2–4] Such critical processes depend on molecules that have to be transported into or out of the nucleus.[3] It is known that the hypertrophic gene programme is activated when HDACs are phosphorylated and exported from the nucleus, and their transcriptional repression relieved, resulting in expression of an MEF2 transcription factor controlled gene programme.[5] Thus, since the nuclear transport has a limited total capacity,[6] it remains unknown how the nuclear transport machinery [transport receptors and nuclear pore complex (NPC)] functions to sustain increased workloads for nucleocytoplasmic trafficking.

The classical nuclear protein import (NPI) cycle is initiated upon nuclear localization sequence (NLS)-containing cargo (proteins

* Corresponding author. Tel: +44 7850587924; fax: +44 2075943009, Email: m.chahine@imperial.ac.uk, mirnachahine01@gmail.com

† G.F. and S.E.H. share the last authorship position in this paper.

© The Author 2014. Published by Oxford University Press on behalf of the European Society of Cardiology.
This is an Open Access article distributed under the terms of the Creative Commons Attribution Non-Commercial License (http://creativecommons.org/licenses/by-nc/4.0/), which permits non-commercial re-use, distribution, and reproduction in any medium, provided the original work is properly cited. For commercial re-use, please contact journals.permissions@oup.com

**Table 1 Abbreviations**

| | |
|---|---|
| AZA | 1-Azakenpaullone |
| BDM | 2,3-Butanedione monoxime |
| CAS | Cellular apoptosis susceptibility |
| CM | Cardiomyocytes |
| CRM1 | Chromosome region maintenance 1 |
| HF | Heart failure |
| hDCM | Human dilated cardiomyopathy |
| LV | Left ventricular |
| LMB | Leptomycin B |
| MI | Myocardial infraction |
| NESs | Nuclear export signals |
| NLS | Nuclear localization sequence |
| NPCs | Nuclear pore complexes |
| NPE | Nuclear protein export |
| NPI | Nuclear protein import |
| NTF2 | Nuclear transport factor 2 |
| PE | Phenylephrine |
| RanGAP | RanGTPase-activating protein |
| RanGEF | Ran Guanine nucleotide Exchange Factor |
| rICM | Rat with ischaemic cardiomyopathy |
| RV | Right ventricular |
| TSA | Trichostatin A |

>40 kDa) recognition by a heterodimeric NLS receptor composed of an 'α' subunit (importin-α) and a 'β' subunit (importin-β), which usher the cargo protein through the NPC with (FG)-nucleoporin (Nup) interaction, such as Nup p62.[7] This energy-dependent process is controlled by a RanGTP/GDP cycle controlled by RanGTPase-activating protein (RanGAP).[7–9] During the classical nuclear protein export (NPE) cycle, the transporter chromosome region maintenance 1 (CRM1) or Exportin-1 recognizes proteins in the nucleus containing nuclear export signals (NESs). The complex CRM1/NES-containing cargo protein/RanGTP moves through the NPC via Nup interactions.[10]

Nucleocytoplasmic transport is therefore a highly controlled process and its regulation is modulated by the expression or function of single cargoes, transport receptors, or the transport channel itself.[9] Thus, dysregulation at any level of these targets might have a considerable impact on the capacity of the transport and eventually affecting gene expression, signal transduction, cell growth, and disease.[9] However, there has been little attention to this process in cardiac hypertrophy and failure, with only a few studies on cultured neonatal rat cardiomyocytes (CMs)[3,11,12] or in failing myocardial tissue.[10] Here, we report a down-regulation in NPI and up-regulation in NPE occurring rapidly in adult rat CMs after acute phenylephrine (PE) treatment, and similar established alterations in CMs from failing rat and human heart. Our observations on the control of this process suggest nucleocytoplasmic transport as a novel control point for the development of the hypertrophic phenotype and therefore a therapeutic target for intervention during the stages of cardiac hypertrophy and HF.

# 2. Methods

Refer to the extended methods in Supplementary material online, Materials and Methods for details.

## 2.1 Human ventricular tissue and CM isolation

Human ventricular tissue was obtained from explanted hearts of patients with dilated cardiomyopathy (DCM) at the time of transplant or from unused donor hearts,[13] and CMs were isolated as published previously.[14]

## 2.2 Adult rat ventricular tissue, post-myocardial infarction-HF assessment, and CM isolation

*Rat HF model:* Adult male Sprague–Dawley rats (250–300 g; $n = 5$) underwent proximal coronary ligation. Myocardial infarction (MI) was quantified by planimetry of a mid-left ventricular (LV) section to ensure adequate infarction. Rats underwent echocardiography using a Vevo 770 system and then hearts were explanted and prepared for cell isolation.[13,15]

## 2.3 Use of PE and small molecule inhibitors of hypertrophy

Non-failing adult rat CMs (CT 8w or AMC 16w) were incubated in medium 199 containing 10 μM α-adrenergic PE (Sigma) for 48 h (PE 48 h 8w or PE 48 h 8w, respectively). Selective small molecule inhibitors of p38 MAP kinase [SB202190 (SB; 1 μmol/L)[16]]; HDAC II [(trichostatin A (TSA; 85 nmol/L)[17,18]]; and GSK3β [1-azakenpaullone (AZA; 10 μmol/L)[16]] were only administered to Control rat CM (CT 8w) in the presence or absence of PE for 48 h (PE 48 h 8w). Exportin-1 (CRM1) inhibitor Leptomycin B (LMB; 10 nM) was applied for 4 h on rat CM at the end of the PE incubation or on failing human LV and right ventricular (RV) CM. DMSO was used as control. In microinjection experiments, adult CMs were exposed to a 15-min PE (Acute PE) and a 48-h PE treatment.

## 2.4 Cell microinjection and confocal microscopy

Adult CMs were transferred to a low-$Ca^{2+}$ solution, supplemented with 2,3-butanedione monoxime to inhibit contraction,[19] and microinjection was performed under a confocal microscope.[7,9,20–22]

## 2.5 Nuclei isolation

Adult rat CM nuclei were isolated as published previously with some modifications.[23]

## 2.6 Protein quantification and western blot analysis

Cultured adult rat CMs and isolated nuclei were homogenized. Lysates were diluted in Laemmeli buffer and separated proteins transferred onto PDVF membranes as published previously.[24,25]

## 2.7 Statistical analysis

Results were reported as mean ± SEM or SD as indicated, analysed by unpaired Student's *t*-test or one-way ANOVA followed by a Student–Neuman–Keuls *post hoc* test for multiple comparisons or a two-way ANOVA followed by a Bonferroni *post hoc* test for multiple comparisons (effects of MI and/or age) with $^{*}P < 0.05$, $^{**}P < 0.01$, and $^{***}P < 0.001$ as statistically significant. When results are shown for example as $N = 4–5$ animals; $n = 3$ experiments/animal, then the mean ± SEM is calculated for animals (with cell results averaged to give $n = 1$ per animal). This is the more conservative approach, although may underestimate the significances compared with a hierarchical clustering method.

# 3. Results

## 3.1 Functional indications of hypertrophy in isolated ventricular myocytes

The hypertrophic phenotype of CMs from failing heart is well described.[26] Here, we used a model of chronic HF, developed 1–18 weeks after MI by coronary ligation in the adult rat (rat with ischaemic

cardiomyopathy, rICM). CMs isolated from the hearts of rICM showed significant increases in cell and nuclear sizes compared with age-matched controls (*Figure 1A–C*). Hypertrophy was established at 4 weeks after MI, as evidenced by heart weight/tibial length (HW/TL); a two- way ANOVA showed an overall significant difference in MI (compared with AMC; $P < 0.05$) on the HW/TL (see Supplementary material online, *Figure S1*); changes in cell length and width (see Supplementary material online, *Figure S2*) and in nuclear area (see Supplementary material online, *Figure S3*). Evidence of HF, with progressive deterioration of ejection fraction and appearance of ventricular dilation (see Supplementary material online, *Figure S1*), was seen at 16 weeks. Indeed, a two- way ANOVA showed significant effects of MI (compared with AMC; $P < 0.01$) and age (between 4 and 16 weeks; $P < 0.01$) on fractional shortening (FS; see Supplementary material online, *Figure S1*). There were also statistically significant effects on LV end-diastolic dimension of MI (compared with AMC) ($P < 0.05$ at 4 weeks after MI compared with 4 weeks AMC; $P < 0.01$ at 16 weeks after MI compared with 16 weeks AMC) and age (between 4 and 16 weeks; $P < 0.01$; see Supplementary material online, *Figure S1*). We have previously described in detail the increase in size in CM from human ventricle with failure of various aetiologies,[26] and cell and nuclear sizes in a further set of CM from patients with idiopathic-dilated cardiomyopathy (hDCM) are displayed in *Figure 1A–C*. In the present study, we had matched frozen tissue from non-failing human heart. Nuclear sizes determined from

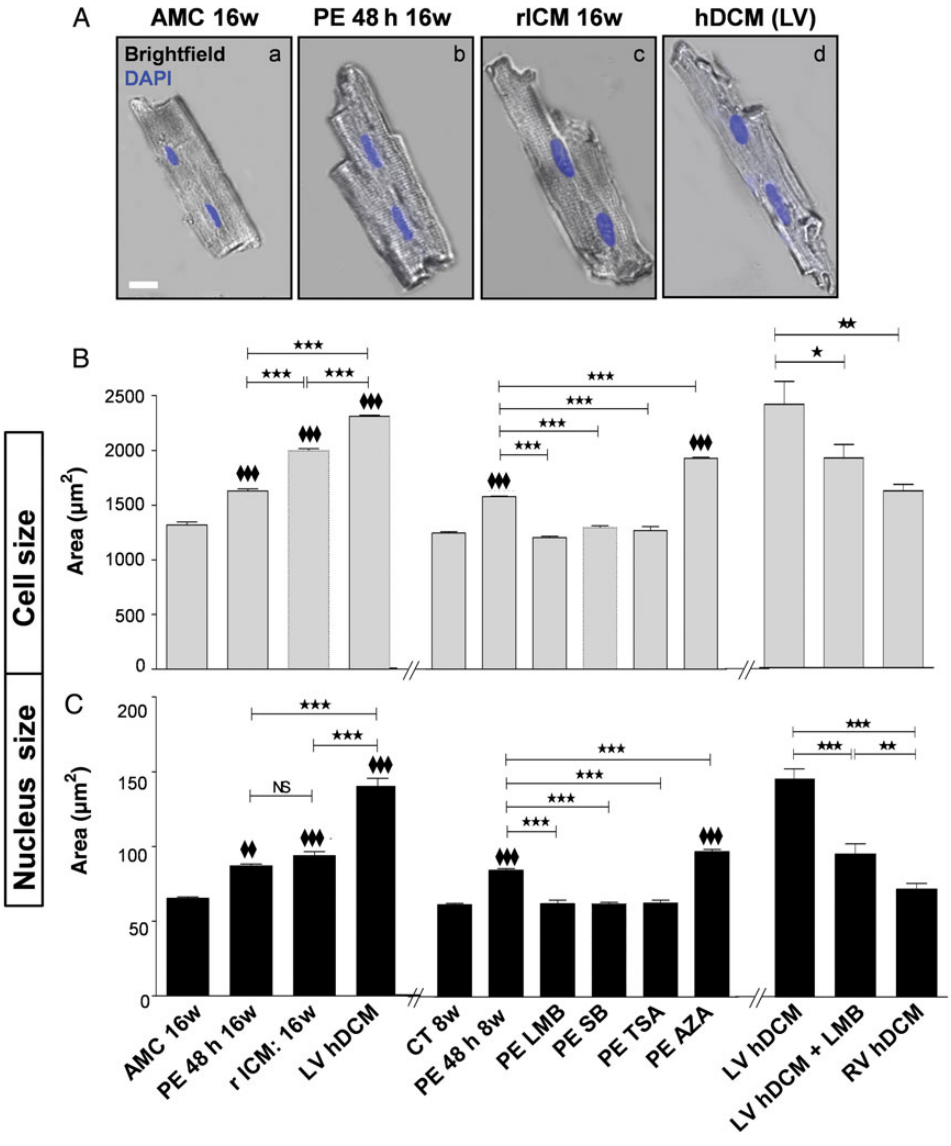


**Figure 1** Increase in cell and nuclei sizes in PE-treated adult rat CMs. Failing rat and LV human CMs have similarly increased sizes. (*A*) Representative merged brightfield images with nuclei stained with DAPI (blue) showing 16w AMC healthy rats' CM: AMC 16w (a) treated with PE: PE 48 h 16w (b), failing rat CM: rICM 16w (c), and failing LV human CM: hDCM (d). Scale bar represents 20 µm. (*B*) and (*C*) Bar graphs (left and right sides) showing cell size (*B*) and nuclear size (*C*) in healthy AMC 16w rat CM in culture for 48 h (AMC 16w) and in healthy 16w AMC rat CM exposed to PE (PE 48 h 16w), as well as in failing rat CM (16w MI) and failing human RV and LV CM from hDCM in the absence or presence for 4 h to LMB. Bar graphs (middle) showing cell size (*B*) and nuclear size (*C*) in healthy rat CM in culture for 48 h (CT 8w) and in healthy rat CM exposed to PE (PE 48 h 8w) in the absence or presence for 48 h of SB, TSA, LMB (4 h only), and AZA. Results are expressed in area ($\mu m^2$) and shown as mean ± SEM ($N = 4–5$ animals; $n = 3$ experiments/animal). NS: non-significant; *$P < 0.05$, ◆◆ and **$P < 0.01$, ◆◆◆ and ***$P < 0.001$; ◆◆ or ◆◆◆ are vs CT8w or vs AMC 16w.

immunohistochemistry of frozen sections were larger in hDCM than in non-failing samples. LV CM from a patient with hDCM showed significant increases in cell and nuclear sizes compared with RV CM (*Figure 1B* and *C*): we have previously shown the cell size difference between ventricles in a larger human cohort.[26] Increased atrial natriuretic factor (ANF) and brain natriuretic peptide (BNP) mRNA levels measured by qPCR were also observed in failing rat CMs and in failing human LV tissue compared with non-failing controls (see Supplementary material online, *Figures S4A* and *S5*).

As an acute hypertrophic model, normal adult rat CMs were subjected to PE treatment for 48 h. They showed significant increases in cell and nucleus sizes (*Figure 1*) and ANF mRNA levels (see Supplementary material online, *Figure S4*). Increases in cell and nuclear sizes (*Figure 1B* and *C*) and ANF mRNA levels (see Supplementary material online, *Figure S4B*) with PE were prevented by p38 inhibitor, SB202190 (SB) and HDAC II inhibitor, TSA. Surprisingly, the nuclear export inhibitor LMB applied for 4 h to rat CM after 44-h incubation of the PE treatment and in LV CM from hDCM was able to significantly decrease cell and nuclear sizes (*Figure 1B* and *C*). This was not an acute effect on cell swelling, since sarcomere length remained constant (Control: $2.05 \pm 0.05$ μm; PE: $2.01 \pm 0.05$ μm; PE + LMB: $2.06 \pm 0.04$ μm, $n = 34$), but numbers of sarcomeres increased with PE (to $157 \pm 4.1\%$ of control, $P < 0.001$) and decreased with PE + LMB (to $108.4 \pm 4.7\%$ of control, $n = 10$). Inhibition of the anti-hypertrophic GSK3β pathway by AZA induced further increases in cell and nuclear sizes (but not ANF levels) compared with PE-treated levels (*Figure 1B* and *C*, and see Supplementary material online, *Figure S4B*).

## 3.2 Live cell NPI assays

Microinjection with an Alexa488-BSA-NLS to visualize an NPI rate in adult CM showed a high level of fluorescence in the cytoplasm (0 min) that was gradually transferred into the nucleus of the cells (5 min post-injection) reaching a maximum at 15 min post-injection (*Figure 2Ab–d*). Exposure to PE for 48 h decreased both rate and maximum extent of fluorescent transfer by NPI (*Figure 2*; $P < 0.001$). To determine how rapidly this could occur, NPI was measured after shorter exposures of CM to PE, and it was found that 15 min treatment was sufficient to induce a significant decrease (*Figure 2A–C*).

NPI was low in 16-week-old rICM, and the decrease was evident before the development of HF, at 4 or 8 weeks (*Figure 2C*) compared with healthy AMC rat CM (4w, 8w, and 16w, respectively). Note that no difference was found in import between CM isolated from AMC 4w, AMC 8w, or AMC 16w healthy rat CM. In CM isolated from hDCM, the import was low compared with AMC 4w or AMC 8w or AMC 16w healthy rat CM, but non-failing human CMs were not available (*Figure 2C*). Interestingly, LV CM from hDCM showed significantly lower NPI than the less hypertrophied RV CM (*Figure 2C*). Inhibitors SB or TSA, but not AZA, prevented the decrease in NPI in CM exposed to PE for 48 h (*Figure 3*). LMB added for 4 h to CM at the end of the PE treatment (*Figure 3*) or, importantly, to LV CM from hDCM (*Figure 3B*) was able to significantly increase the NPI to levels seen in normal rat CMs or in RV CMs.

## 3.3 Expression and localization of components of the nuclear import/export complexes

Localization was determined through immunohistochemical staining of heart sections or isolated myocytes and western blotting of purified nuclear fractions. Nup p62 relative density was significantly decreased in the nucleus of hDCM (*Figure 4A* and *B*) and failing rat heart sections compared with non-failing controls (see Supplementary material online, *Figure S4A*), and the same was seen in isolated myocytes (*Figure 4D*). Exposure adult rat CMs to PE for 48 h induced a significant diminution in the p62 relative density (*Figure 4C* and *D*) and protein expression levels assessed by western blot (*Figure 4E* and *F*). SB, TSA, and LMB, but not AZA, normalized the PE-induced decrease in p62 relative density and protein expression levels.

Nuclear translocation of transport receptor importin-β was significantly decreased in hDCM (*Figure 5A* and *B*) and rICM heart sections compared with non-failing controls (see Supplementary material online, *Figure S6B*). RanBP1 relative density was decreased in the cytoplasm in hDCM and rICM heart CMs (*Figure 5B* and *C*) and rat ventricular tissue (see Supplementary material online, *Figure S6C*). This would lead to a decreased level of importins to be shuttled into the cytoplasm and therefore to a decreased NPI. A significantly lower ratio of nuclear over cytoplasmic relative density of importin-α and -β was observed in isolated CM from hDCM and rICM (*Figure 5D*). Conversely, the ratio of cytoplasmic over nuclear (C/N) relative density of RanBP1 was decreased in hDCM and rICM CMs (*Figure 5D*).

Similarly, exposure of adult rat CM to PE for 48 h significantly decreased importin-α and -β N/C and also Ran BP1 C/N (*Figure 5C* and *D*). Following cell fractionation, N/C protein levels of importin-α and -β (*Figure 6B* and *C*) were significantly decreased in CM exposed to PE. The inhibitors SB, TSA, and LMB, but not AZA, normalized the decrease in density (*Figure 5C* and *D*) and expression levels (*Figure 6*) of importin-α, importin- β, and RanBP1 in CM exposed to PE for 48 h.

Nuclear export of CRM1 was significantly increased in tissue from hDCM and rICM (*Figure 7A*), as well as in isolated CM from hDCM and rICM (*Figure 7C*). Likewise, exposure of adult rat CM to PE for 48 h induced a significant increase in the C/N fluorescence levels of CRM1 (*Figure 7B* and *C*). Following cell fractionation, protein C/N levels of CRM1 were significantly increased in CM exposed to PE for 48 h (*Figure 7D* and *E*). Exposure of CM to SB, TSA, and LMB, but not AZA, normalized the increase in relative density (*Figure 7C*) and expression levels (*Figure 7E*) of CRM1 in CM exposed to PE for 48 h, but had no significant effect in control cells (see Supplementary material online, *Figure S7*).

# 4. Discussion

NPI and NPE are tightly associated as they compete for the same routes, via the central channel of the NPC,[3] so that the increased export when necessary for *de novo* protein synthesis during hypertrophy must be linked to decreased import to be sustainable. In the failing human heart tissue and CM studied, here we saw evidence of this reciprocal shift, with increased CRM1 for export, decreased Nup 62 for import, reorganization of the import transport receptors, and low uptake of fluorescent NLS-linked substrate. This is the first study in which microinjection has been used to introduce NLS substrate to an adult CM of any species. The rat MI/HF model has been well characterized before.[13,24,27] Time points were chosen to distinguish between compensated hypertrophy (4w) and decompensated failure (16w). Hypertrophy was well established by 4w in terms of increase in cardiomyocyte length and width (see Supplementary material online, *Figures S1* and *S2*), but there was no increase in end-diastolic dimension. FS was decreased (see Supplementary material online, *Figure S1*), but was considered to be the largely the initial result of the infarct. By 16w, cardiomyocyte

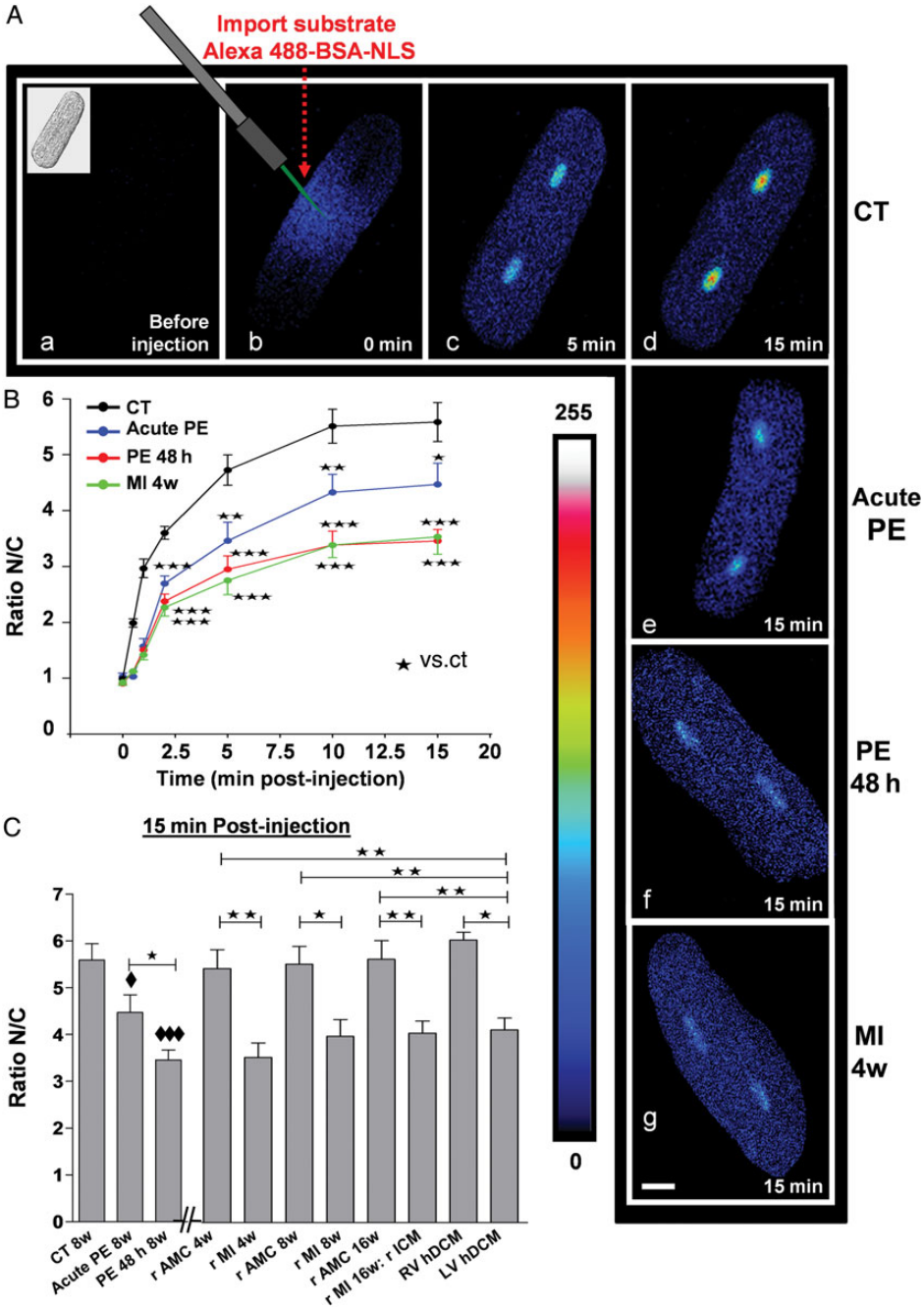


**Figure 2** NPI in live CM. Effect of shorter and longer PE treatment on adult rat CM to decrease NPI. Comparison with CM from failing rat (MI 4, 8, and 16 weeks) and CM from LV failing human hearts (hDCM). (*A*) Representative confocal images of adult rat CM microinjected with an import substrate following a shorter (acute PE: for 15 min) (e) or a longer exposure to PE (48 h) (f) or in failing rat CM (4w MI) (g) or in control cells (a–d). Images were taken at 0 min pre-injection accompanied with a brightfield image of the CM (upper left corner) (a), 0 min post-injection (b), 5 min post-injection (c), and 15 min post-injection (d). (e–h) were taken at 15 min post-injection. The pseudocolour scale represents fluorescence intensity levels from 0 (black colour) to 255 nm (white colour). The white size scale bar is 20 μm. Laser scanning settings are identical for all cells and experiments. (*B*) The curves summarize the NPI in CM exposed to the same conditions as in (*A*). (*C*) The bar graph summarizes the NPI in rat CM (CT 8w) and in CM exposed for a short (acute PE 8w) and a long (PE 48 h 8w) period to PE or untreated CM from 4w, 8w, 16w rMI, and their respective AMC (4w, 8w, and 16w), LV and RV hDCM at 15 min post-injection (*C*). Values are means ± SEM ($N = 4$ animals; $n = 4–10$ cells/animal). ◆ and *$P < 0.05$, **$P < 0.01$, ◆◆◆ and ***$P < 0.001$; ◆ vs. CT 8w.

hypertrophy had not progressed further, but HW/TL ratio was now significantly increased, FS had deteriorated markedly, and end-diastolic dimension was significantly increased. We show here increases in cell and nuclear sizes and ANF levels similar in direction to those seen in the failing human samples. In addition, the detailed changes in import and export components paralleled those observed in the human CM, including the low uptake of NLS-linked substrate. Changes in NLS substrate uptake after rat MI were seen as early as 4w after the

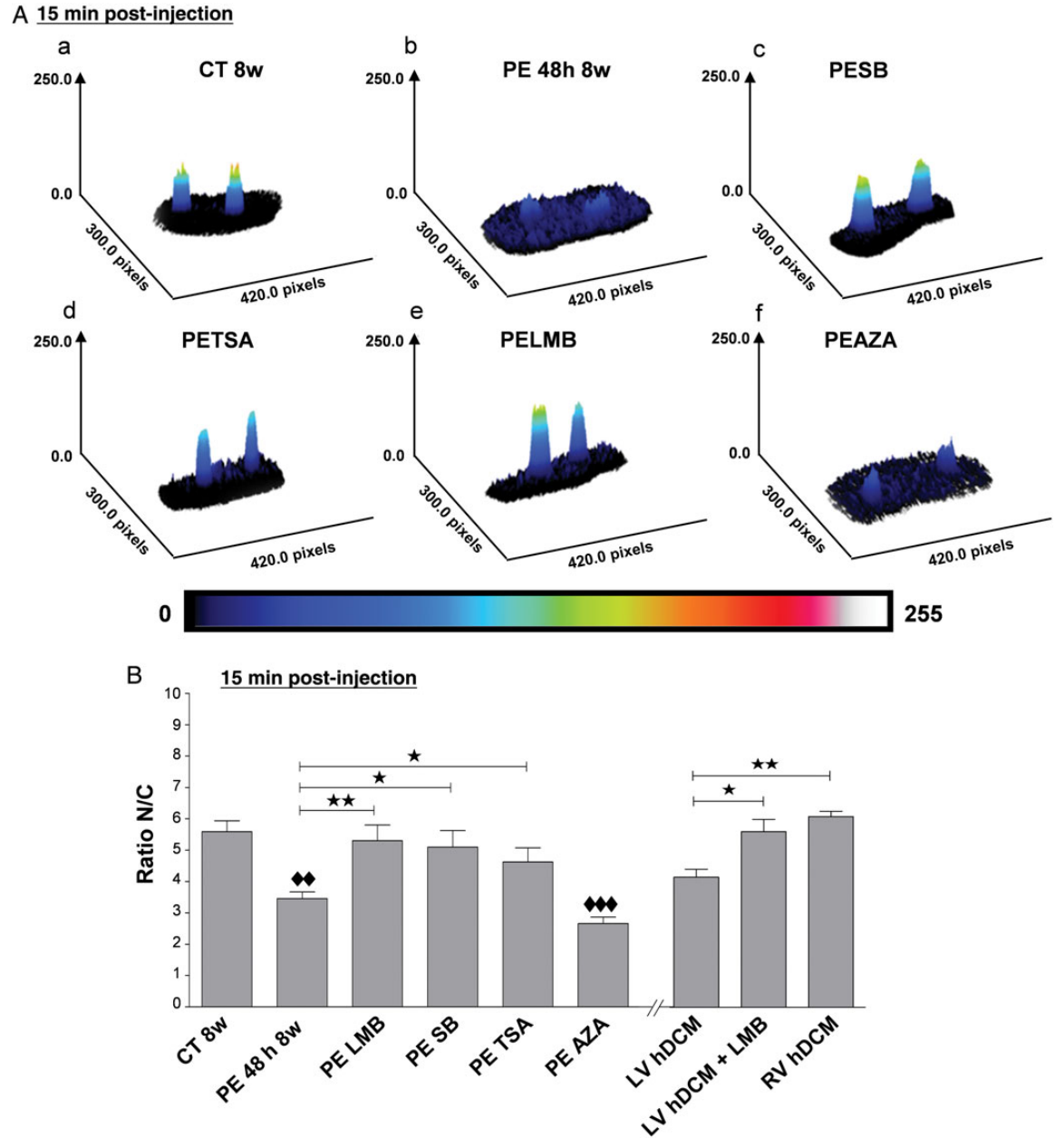


**Figure 3** The alteration of NPI is p38 MAPK, HDAC II, and CRM1 pathways-dependent in PE-treated rat adult rat CMs and CRM1 pathway-dependent in LV hDCM CMs. Representative 3D projection images (*A*) and bar graph (*B*) show the alteration of NPI in adult rat CM microinjected with an import substrate in rat control CM (CT 8w) (a) and in rat CM exposed to PE for 48 h (PE 48 h 8w) in the absence (b) or presence of SB202190 (PESB) (c), TSA (PETSA) (d), LMB (PELMB) (e), and AZA (PEAZA) (f) and in LV hDCM CM in the absence or presence of LMB at 15 min post-injection. In (*A*), the pseudocolour scale represents fluorescence intensity levels from 0 (black colour) to 255 nm (white colour). (*B*) Results are expressed as the ratio nuclear fluorescence (N)/cytoplasmic fluorescence (C). Values are means ± SEM ($N = 4$ animals; $n = 4$–10 cells/animal). *$P < 0.05$, ◆◆ and **$P < 0.01$, ◆◆◆$P < 0.001$; ◆◆ or ◆◆◆ are vs CT8w.

operation, putting it as a primary event in the hypertrophic process and prior to HF.

To investigate the mechanisms and time course more fully, we used the α-adrenoceptor agonist PE, a canonical inducer of Gαq-mediated pathological hypertrophy.[16,28] Treatment of adult rat CM with PE for 48 h produced robust increases in cell and nuclear sizes and ANF levels, although lower than those in the rat MI model at 16 weeks. Increases in export CM1, decreases in nuclear port import components, reorganization of the import transport receptors, and decreases in uptake of fluorescent NLS-linked substrate were all reproduced simply by exposure to PE. Our data are consistent with inhibition in NPI levels observed in neonatal rat CM exposed to PE or AngII[3] or in medium depleted of cellular $Ca^{2+}$,[11] and suggest that reorganization of nuclear pore control could be an early event in the development of the hypertrophic phenotype. Furthermore, we could detect the first significant changes in NLS substrate uptake after only 15 min of PE exposure, suggesting an effect of a second messenger signalling pathway on component location or

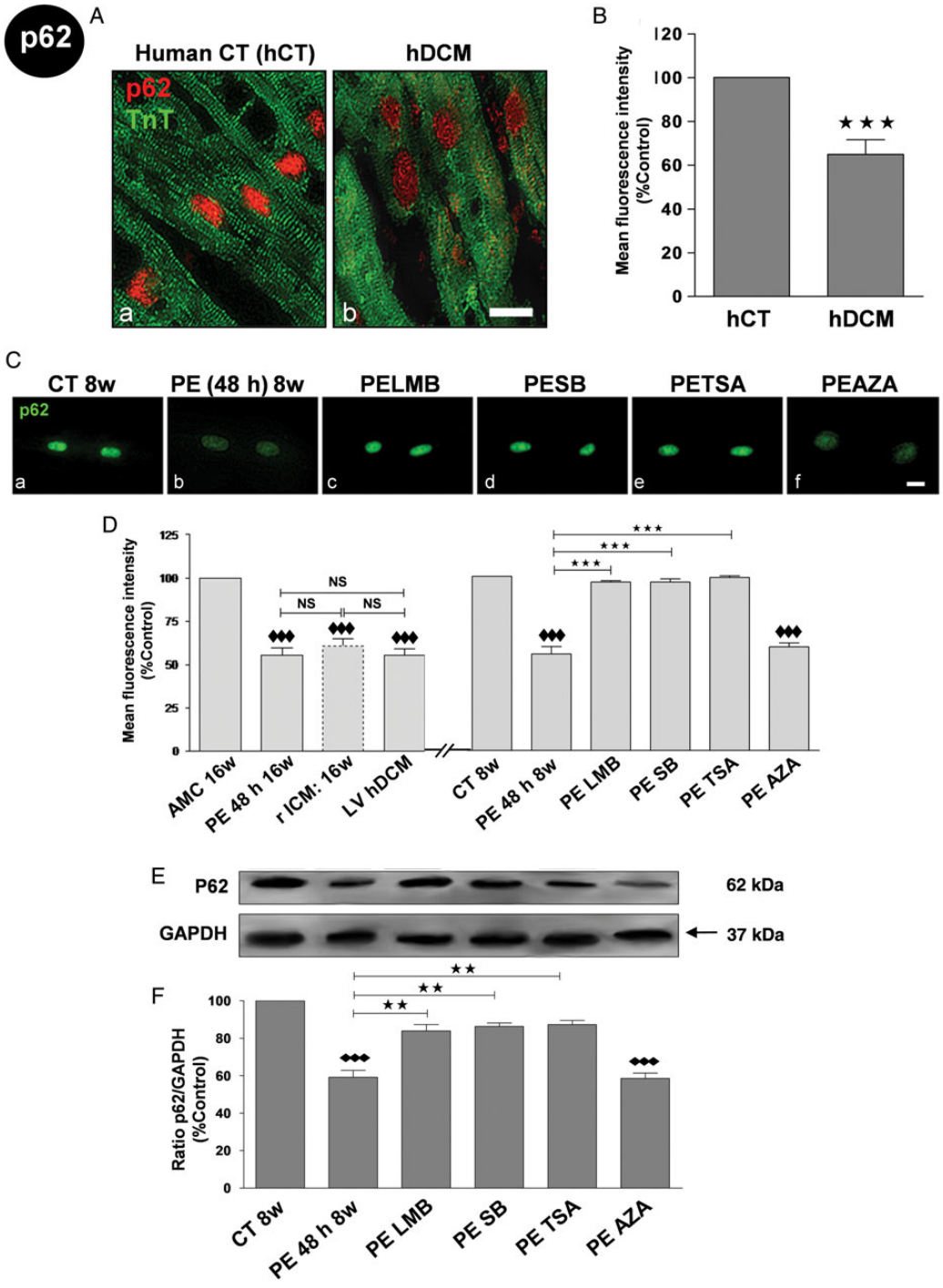


**Figure 4** Decrease relative density and expression of Nup p62 in PE-treated adult rat CM through p38 MAPK, HDAC II, and CRM1, but not GSK3β, pathway(s). Failing rat and human CMs and human ventricular tissue have similarly altered levels. (*A*) Representative IF confocal images showing human heart tissue of (a) healthy donors (hCT) (b) and human with DCM (hDCM) stained for p62 (red) and troponin T (TnT) (green). (*B*) Bar graphs showing mean fluorescence levels (%Control) of p62 levels in HCT (white bar) and hDCM (red). Results are shown as mean ± SEM ($N = 4$ hearts; $n = 3$ experiments/heart). (*C*) Representative IF confocal images of 8w-old rat CM stained with p62 antibody (green) in rat control CM (CT 8w) (a), or in rat CM exposed to PE for 48 h (PE 48 h 8w) in the absence (b) or presence of SB (c), TSA (d), LMB (e), and AZA (f). (*D*) Bar graphs showing the mean fluorescence levels (%Control) of p62 in the nuclei of: (left side) AMC 16w rat CM, MI 16w rat CM, and human CM, and (right side) in rat control CM (CT 8w) exposed to PE (PE 48 h 8w) in the absence or presence of SB, TSA, LMB, or AZA. Results are shown as mean ± SEM ($N = 4$ hearts; $n = 3$ experiments/heart). NS: non-significant. (*E*) Representative western blots and (*F*) analysis by densitometry of p62 expression (%Control) in rat control CM (CT 8w) exposed to PE (PE 48 h 8w) in the absence or presence of SB, TSA, LMB, and AZA. Even sample loading was confirmed by GAPDH detection. Results are shown as the mean of the ratio p62/GAPDH ± SEM ($N = 3$ hearts; $n = 3$ experiments/heart). The white size scale bar is 20 μm. $^{**}P < 0.01$, ♦♦♦ and $^{***}P < 0.001$; ♦♦♦ vs CT8w.

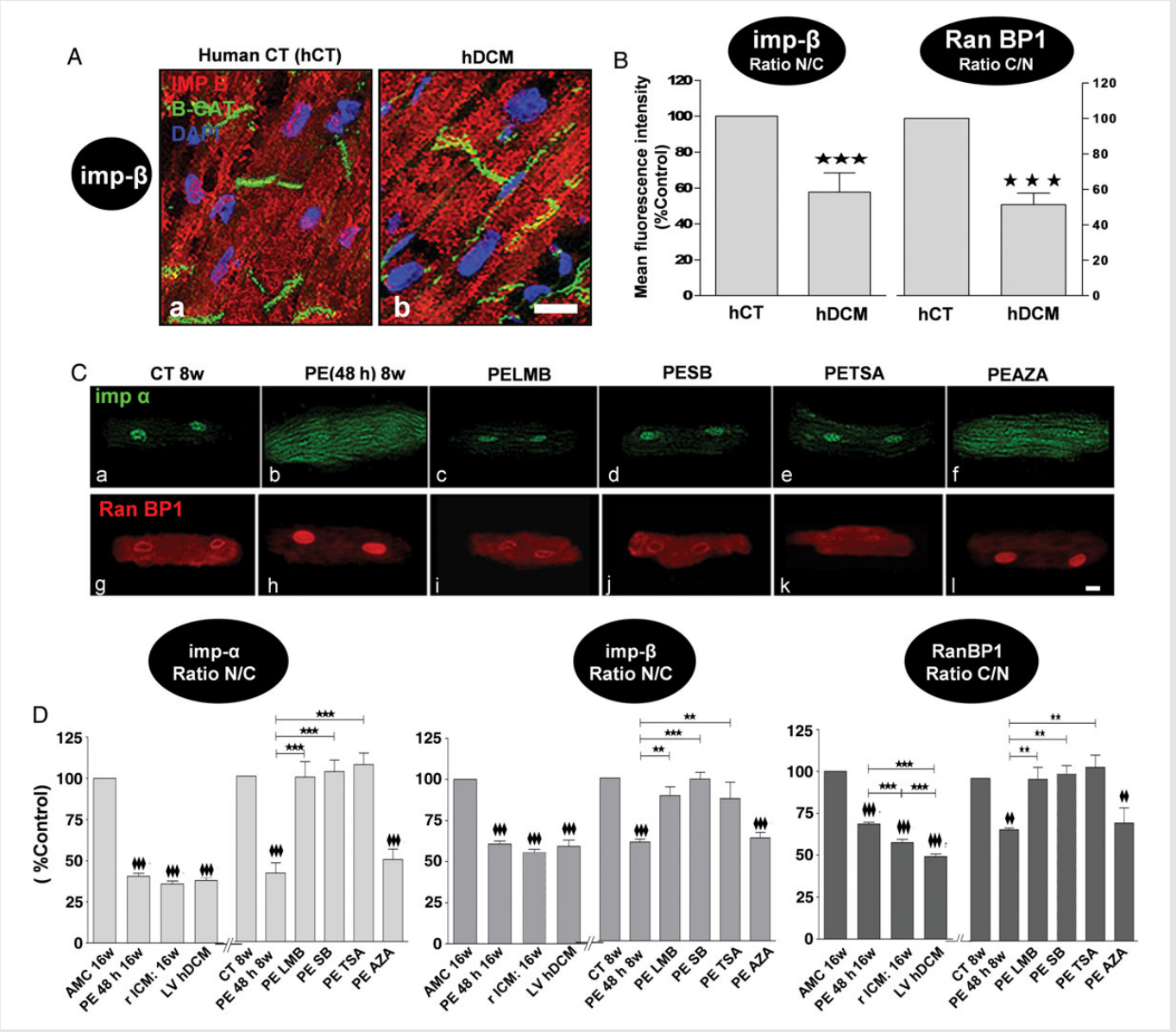


**Figure 5** Decrease in the relative density of nucleocytoplasmic trafficking transport receptors (imp-α and imp-β) and transport driving force protein (RanBP1) in PE-treated adult rat CM through p38 MAPK, HDAC II, and CRM1, but not GSK-3β, pathway(s). Failing rat and human CMs and human ventricular tissue have similarly altered levels. (*A*) Representative IF confocal images showing human heart tissue of (a) healthy donors (hCT) and (b) human with DCM (hDCM) stained for importin-β (Imp-β) (red), β-catenin (β-Cat) (green), and DAPI for nuclei (blue). (*B*) Bar graphs showing the ratio of nuclear/cytoplasmic (N/C) mean fluorescence intensity (%Control) of Imp- β (left) and the ratio of cytoplasmic/nuclear (C/N) mean fluorescent intensity of RanBP1 (right) in hCT (white bar) and hDCM (red). Results are shown as mean ± SEM ($N = 4$ hearts; $n = 3$ experiments/heart). (*C*) Representative IF confocal images of rat CM stained with Imp-α antibody (green; a–f) and RanBP1 (red; g–l) in rat control CM (CT 8w) (a, g), or in rat control CM exposed to PE (PE 48 h 8w) in the absence (b, h) or presence of SB (c, i), TSA (d, j), LMB (e, k), and AZA (f, l). (*D*) Bar graphs showing mean fluorescence intensity levels (%Control) of Imp-α, Imp-β, and RanBP1 in AMC 16w rat CM and MI 16w rat CM (rICM), and hDCM, as well as rat control CM (CT 8w) exposed to PE (PE 48 h 8w) in the absence or presence of SB, TSA, LMB, and AZA. Results are shown as mean ± SEM ($N = 4–5$ hearts; $n = 3$ experiments/heart). The white size scale bar is 20 μm. ◆◆ and $^{**}P < 0.01$, ◆◆◆ and $^{***}P < 0.001$; ◆◆ or ◆◆◆ are vs CT8w or vs AMC 16w.

activity rather than a necessary change in expression levels as an initiating process.

We used small molecule inhibitors to elucidate the involvement of several pathways in PE-induced or pathological hypertrophy such as HDAC II[17,18] or p38 MAPK,[16] chosen because they had given strong signals against PE in our human stem cell screen.[16] The role of the p38 MAPK inhibitor had been verified by siRNA knockdown and overexpression of a dominant negative construct in that study. However, we note that the evidence for p38 MAPK involvement in hypertrophy in the adult rat cardiomyocyte is controversial. p38 MAPK has been implicated in hypertrophy in a range of cell and animal models, and inhibitors of p38 MAPK shown to reduce hypertrophic growth.[29–33] However, transgenic overexpression or knockout has rather shown that p38 MAPK suppresses rather than produces hypertrophy,[34] and later studies implicated PI3 kinase and p110α in the hypertrophic signalling stimulated by αAR.[35]

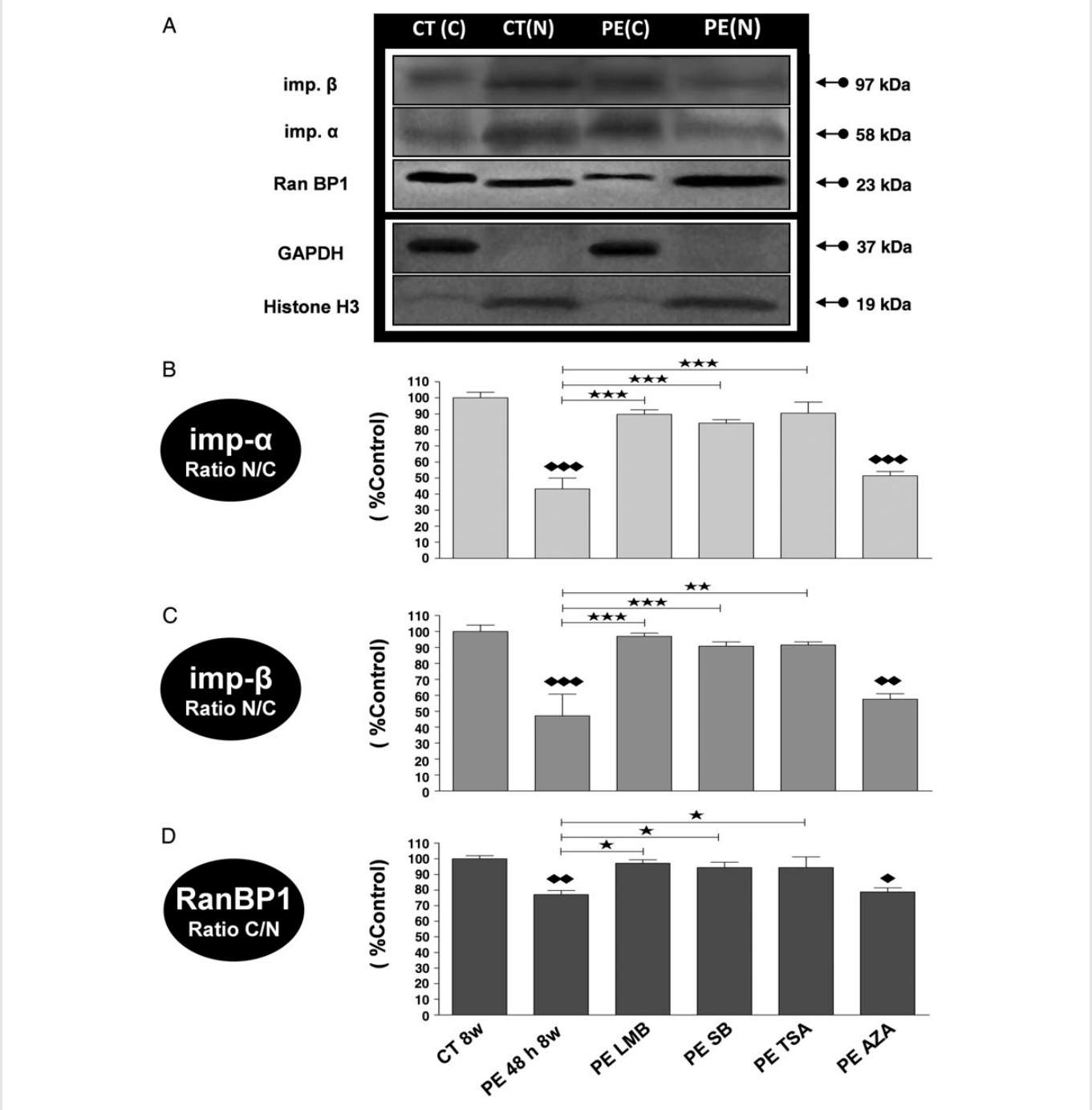


**Figure 6** Alteration in the expression of cytosolic and nuclear transport receptors (Imp-α and Imp-β) and transport driving force protein (RanBP1) in PE-treated adult rat CM through p38 MAPK, HDAC CL II, and CRM1, but not GSK-3β pathway activation. Representative western blots (*A*) and analysis by densitometry of Imp-α (*B*), Imp-β (*C*), and RanBP1 (*D*) expressions in the nuclear and cytosolic fractions of rat control CM (CT 8w) exposed to PE (PE 48 h 8w) in the absence or presence of SB, TSA, LMB, and AZA. Even sample loading of nuclear fractions was confirmed by Histone H3 detection and cytosolic fractions by GAPDH detection. As for equal sample loading between nuclear and cytosolic fractions together, this was performed by staining the blots with Coomassie blue. Results are expressed in percent control and are shown as mean ± SEM ($n = 3$); * and $^{\blacklozenge}P < 0.05$, ** and $^{\blacklozenge\blacklozenge}P < 0.01$, *** and $^{\blacklozenge\blacklozenge\blacklozenge}P < 0.001$; $^{\blacklozenge}$ or $^{\blacklozenge\blacklozenge}$ or $^{\blacklozenge\blacklozenge\blacklozenge}$ are vs CT8w.

Ultimately though, the p38 inhibitors did reduce both cell size and ANP increases in the experiments reported here, and this paralleled the effects on nuclear import. In addition, we had similar data from the HDAC inhibitor to support our conclusions. Blocking these pathways with TSA or SB normalized nuclear pore expression, restored the inhibition in NPI, and reversed redistribution of the transport receptors. This occurred in parallel with normalizing ANF levels and cell/nuclear sizes in adult rat CMs. The results with SB are consistent with previous studies that have shown that nucleocytoplasmic trafficking is sensitive to MAPK activation.[20,21,36] The HDAC II inhibitor, TSA, has been reported

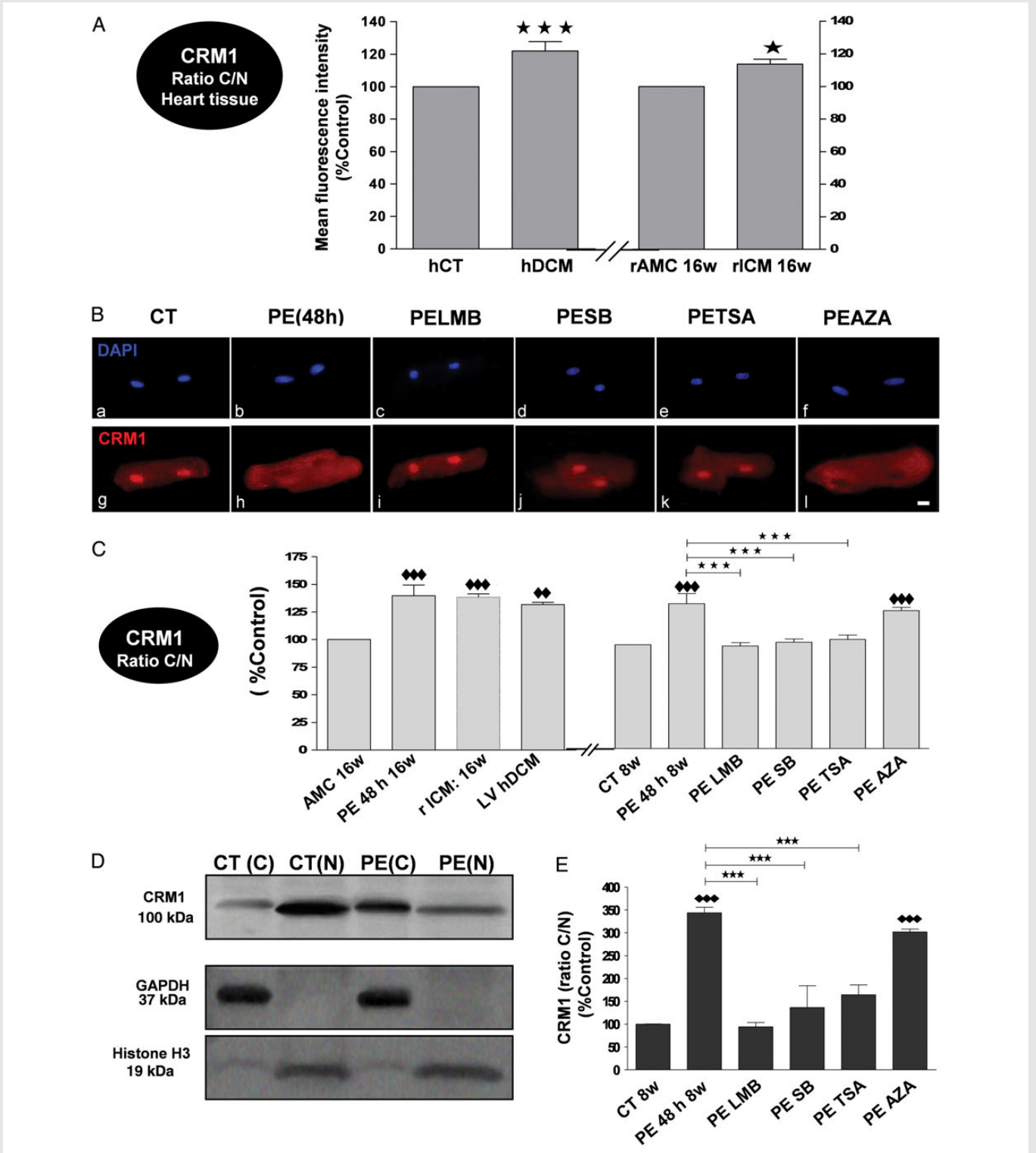


**Figure 7** Increase in CRM1 export in PE-treated adult rat CM through p38 MAPK, HDAC II, and CRM1, but not GSK-3β, pathway(s). Failing rat and human CMs and ventricular tissue (VT) have similarly altered levels. (*A*) Bar graphs showing the ratio C/N mean fluorescence intensity (%Control) of CRM1 in control (hCT: white bar) and failing (hDCM: red) human VT and in control (rat age-matched control: rAMC: white bar) and failing (rICM: red bar) rat VT ($N = 4$ hearts; $n = 3$ experiments/heart). (*B*) Representative IF confocal images of rat CM stained with DAPI (blue; a–f) and CRM1 antibody (red; g–l) in rat control CM (CT 8w) (a, g), or in rat control CM exposed to PE (PE 48 h 8w) in the absence (b, h) or presence of inhibitors. The white size scale bar is 20 μm. (*C*) Bar graphs showing mean fluorescence intensity levels (%Control) of CRM1 in AMC 16w rat CM and MI 16w rat CM (rICM), and hDCM, as well as in rat control CM (CT 8w) exposed to PE (PE 48 h 8w) in the absence or presence of inhibitors ($N = 4$–5 hearts; $n = 3$ experiments/heart). Representative western blots (*D*) and analysis by densitometry (%Control) of CRM1 expression (*E*) in the nuclear and cytosolic fractions of rat adult CM exposed to PE (48 h) in the absence (*D* and *E*) or presence of inhibitors (*E*). All results are shown as mean ± SEM. $^{*}P < 0.05$, $^{\blacklozenge\blacklozenge}P < 0.01$, $^{\blacklozenge\blacklozenge\blacklozenge}$ and $^{***}P < 0.001$; $^{\blacklozenge\blacklozenge}$ or $^{\blacklozenge\blacklozenge\blacklozenge}$ are vs CT8w or vs AMC 16w.

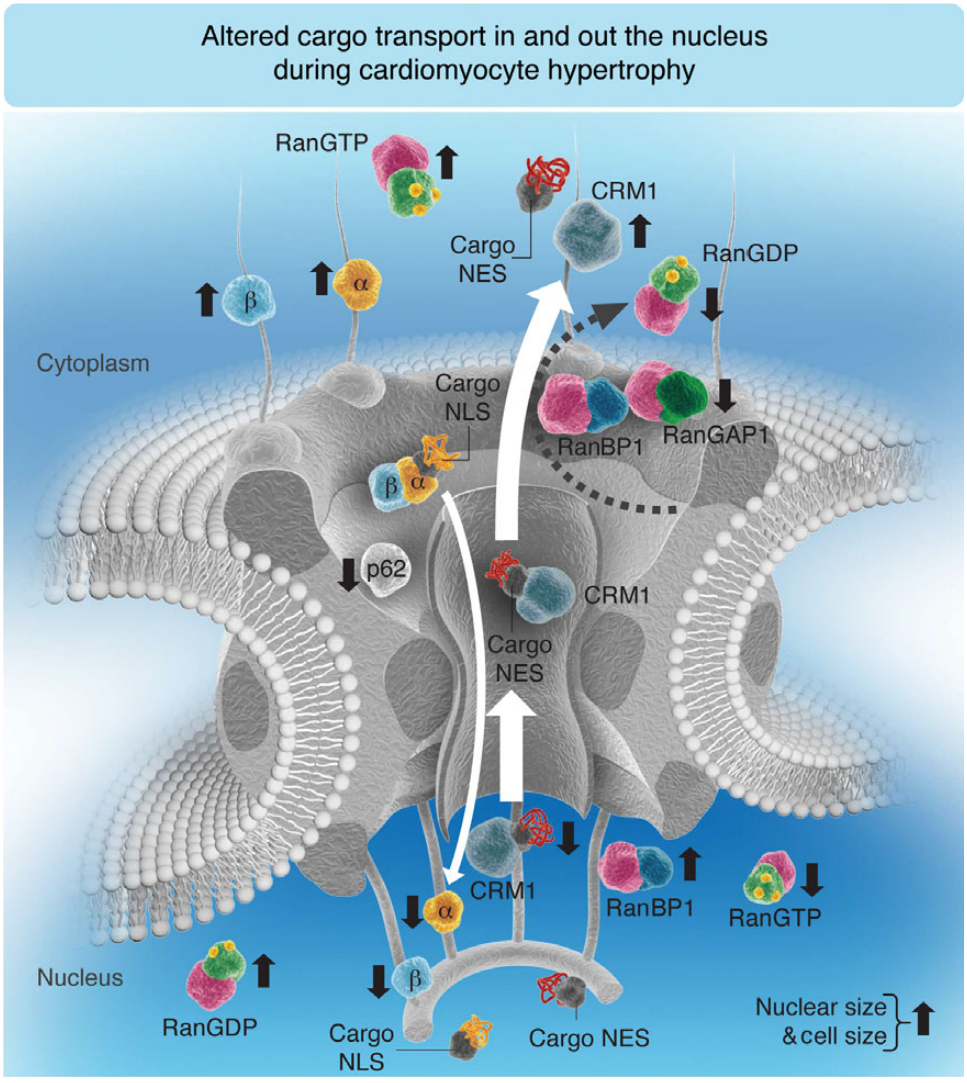


**Figure 8** Hypothetical model occurring in myocardial tissue and isolated CM under hypertrophic conditions. Compared with healthy control (CT) rat CM or healthy human myocardial tissue, the balance between NPI and NPE is disrupted in rat CM exposed to PE for 48 h or with ischaemic cardiomyopathy (rICM) or human cardiac tissue with DCM; under these hypertrophic stimuli, the demand for the nuclear export of transcription factors is exaggerated so that the export receptor (CRM1) is found to be constantly in the cytoplasm. Subsequently, RanBP1, which facilitates the GTP hydrolysis with RanGAP1, cannot be translocated into the cytoplasm by CRM1, and the other import transport receptors (importins-α and -β) are found sequestered in the cytoplasm with RanGTP. Thus, no importins are available in the nucleus to be recycled and released free in the cytoplasm for another import cycle, which can explain the decrease in NPI. In conclusion, under hypertrophic conditions where nuclear and cell sizes are increased, CRM1 cytoplasmic translocation is increased, whereas cytoplasmic RanBP1, Nup p62, and nuclear translocation of importins (α and β) are decreased. The size of the white arrow is proportional to the transport rate. An upward black arrow shows an increase, whereas a downward black arrow shows a decrease. (Note that for simplification, some transport machinery components such as CAS, RanGEF, and NTF2 are not included in this schematic representation since this model is mostly summarizing the elements mentioned in this paper.)

to alter the chromatin association with Nups at the NPC for several gene loci[37] and so may have retained HDAC II intimately linked to Nup p62 in the nucleus. This would prevent Nup down-regulation and subsequent NPI inhibition, as well as repressing MEF2-dependent transcription and NFAT target gene expression.

Blocking CRM1 nuclear export pathways with LMB in hypertrophied CM restored the inhibition in NPI by normalizing Nup p62 expression and relocalizing the protein RanBP1 to the cytoplasm, thus favouring the transport receptor importins-α and -β to be recycled and released for another import cycle and to be relocalized into the nucleus. In addition, and most importantly, LMB was able to reverse cellular hypertrophy in PE-treated adult rat CM [foetal genes (ANF) mRNA levels, and nuclear and cellular sizes]. The effect of LMB on cell size here is consistent with previous studies.[3,25,38] The effect we saw was a true reversal, rather than prevention, since LMB was added at the end of the PE incubation. This result is consistent with the view that increased nuclear export is the key variable linked to hypertrophy, and reduced import is a secondary phenomenon. Interestingly, a decrease in NPI in CM from LV of rat or human failing heart was also reversed after 4 h treatment of LMB (*Figure 3B*), as well as changes in cell and nuclear size,

suggesting that a hypertrophy which has developed over months or years is also amenable to treatment.

In summary, as nuclear export and import share the same transport pathway through the nuclear pore, CM suppress NPI under conditions of increased demand for nucleocytoplasmic communication to secure the availability of the nuclear export transport pathways required for the generation of the hypertrophic phenotype (*Figure 8*). Activation of Gαq pathways is sufficient to rapidly produce the concerted changes in CM nuclear machinery that are observed during the development of HF in a rat model of MI, and in failing human heart. Pathological hypertrophy has been the subject of years of intense research, but has become clear that hypertrophic signalling has multiple pathways and redundancies which may explain why no therapeutic compounds have yet achieved clinically applicability. Since nuclear transport is an integrative control point for all pathways, which act through induction of hypertrophic genes, it may represent a further target for therapeutic development.

# Supplementary material

Supplementary material is available at *Cardiovascular Research* online.

## Acknowledgements

We acknowledge the FILM facility at Imperial College for providing access to the state-of-the-art microscopy equipment and all training and assistance required for the realization of the present study.

**Conflict of interest:** none declared.

## Funding

M.N.C. was supported by a Newton International Fellowship from the British Royal Society. G.F. was supported by British Heart Foundation (BHF), Wellcome Trust Value in People Award, Hungarian Scientific Research Fund, and National Development Agency. M.M. was supported by the NC3Rs and Rosetree's Trust, M.B.S. was supported by the Wellcome Trust (WTN092852), and A.R.L. by the BHF (FS/11/67/28954).

## References

1. Zhang QJ, Chen HZ, Wang L, Liu DP, Hill JA, Liu ZP. The histone trimethyllysine demethylase JMJD2A promotes cardiac hypertrophy in response to hypertrophic stimuli in mice. *J Clin Invest* 2011;**121**:2447–2456.
2. Hill JA, Olson EN. Cardiac plasticity. *N Engl J Med* 2008;**358**:1370–1380.
3. Perez-Terzic C, Gacy AM, Bortolon R, Dzeja PP, Puceat M, Jaconi M, Prendergast FG, Terzic A. Directed inhibition of nuclear import in cellular hypertrophy. *J Biol Chem* 2001;**276**:20566–20571.
4. Kehat I, Molkentin JD. Molecular pathways underlying cardiac remodeling during pathophysiological stimulation. *Circulation* 2010;**122**:2727–2735.
5. Olson EN, Schneider MD. Sizing up the heart: development redux in disease. *Genes Dev* 2003;**17**:1937–1956.
6. Görlich D, Mattaj IW. Nucleocytoplasmic transport. *Science* 2003;**271**:1513–1518.
7. Faustino RS, Cheung P, Richard MN, Dibrov E, Kneesch AL, Deniset JF, Chahine MN, Lee K, Blackwood D, Pierce GN. Ceramide regulation of nuclear protein import. *J Lipid Res* 2008;**49**:654–662.
8. Faustino RS, Stronger LN, Richard MN, Czubryt MP, Ford DA, Prociuk MA, Dibrov E, Pierce GN. RanGAP-mediated nuclear protein import in vascular smooth muscle cells is augmented by lysophosphatidylcholine. *Mol Pharmacol* 2007;**71**:438–445.
9. Chahine MN, Pierce GN. Therapeutic targeting of nuclear protein import in pathological cell conditions. *Pharmacol Rev* 2009;**61**:358–372.
10. Cortés R, Roselló-Lletí E, Rivera M, Martínez-Dolz L, Salvador A, Azorín I, Portolés M. Influence of heart failure on nucleocytoplasmic transport in human cardiomyocytes. *Cardiovasc Res* 2010;**85**:464–472.
11. Perez-Terzic C, Gacy AM, Bortolon R, Dzeja PP, Puceat M, Jaconi M, Prendergast FG, Terzic A. Structural plasticity of the cardiac nuclear pore complex in response to regulators of nuclear import. *Circ Res* 1999;**84**:1292–1301.
12. Hallhuber M, Burkard N, Wu R, Buch MH, Engelhardt S, Hein L, Neyses L, Schuh K, Ritter O. Inhibition of nuclear import of calcineurin prevents myocardial hypertrophy. *Circ Res* 2006;**99**:626–635.
13. Lyon AR, MacLeod KT, Zhang Y, Garcia E, Kanda GK, Lab MJ, Korchev YE, Harding SE, Gorelik J. Loss of T-tubules and other changes to surface topography in ventricular myocytes from failing human and rat heart. *Proc Natl Acad Sci USA* 2009;**106**:6854–6859.
14. Harding SE, Jones SM, O'Gara P, del Monte F, Vescovo G, Poole-Wilson PA. Isolated ventricular myocytes from failing and non-failing human heart; the relation of age and clinical status of patients to isoproterenol response. *J Mol Cell Cardiol* 1992;**24**:549–564.
15. Harding SE, Vescovo G, Kirby M, Jones SM, Gurden J, Poole-Wilson PA. Contractile responses of isolated adult rat and rabbit cardiac myocytes to isoproterenol and calcium. *J Mol Cell Cardiol* 1988;**20**:635–647.
16. Földes G, Mioulane M, Wright JS, Liu AQ, Novak P, Merkely B, Gorelik J, Schneider MD, Ali NN, Harding SE. Modulation of human embryonic stem cell-derived cardiomyocyte growth: a testbed for studying human cardiac hypertrophy? *J Mol Cell Cardiol* 2010;**50**:367–376.
17. McKinsey TA, Kass DA. Small-molecule therapies for cardiac hypertrophy: moving beneath the cell surface. *Nat Rev Drug Discov* 2007;**6**:617–635.
18. Heineke J, Molkentin JD. Regulation of cardiac hypertrophy by intracellular signalling pathways. *Nat Rev Mol Cell Biol* 2006;**7**:589–600.
19. Bartoli M, Claycomb WC. Transfer of macromolecules into living adult cardiomyocytes by microinjection. *Mol Cell Biochem* 1997;**172**:103–109.
20. Richard MN, Deniset JF, Kneesh AL, Blackwood D, Pierce GN. Mechanical stretching stimulates smooth muscle cell growth, nuclear protein import, and nuclear pore expression through mitogen-activated protein kinase activation. *J Biol Chem* 2007;**282**:23081–23088.
21. Chahine MN, Blackwood DP, Dibrov E, Richard MN, Pierce GN. Oxidized LDL affects smooth muscle cell growth through MAPK-mediated actions on nuclear protein import. *J Mol Cell Cardiol* 2009;**46**:431–441.
22. Chahine MN, Dibrov E, Blackwood DP, Pierce GN. Mechanical stretch enhances the oxidized LDL-induced growth, nuclear import and nuclear pore expression of smooth muscle cells through induction of endogenous HSP60 and $ERK_{1/2}$ activation. *Can J Plant Protect* 2012;**90**:1559–1568.
23. Hasegawa Y, Iizuka-Kogo A, Akiyama T, Senda T. High expression of Pitx-2 in the ICAT-deficient metanephros leads to developmental arrest. *Acta Histochem Cytochem* 2010;**43**:51–59.
24. Lyon AR, Bannister ML, Collins T, Pearce E, Sepehripour AH, Dubb SS, Garcia E, O'Gara P, Liang L, Kohlbrenner E, Hajjar RJ, Peters NS, Poole-Wilson PA, Macleod KT, Harding SE. SERCA 2a gene transfer decreases sarcoplasmic reticulum calcium leak and reduces ventricular arrhythmias in a model of chronic heart failure. *Circ Arrhythm Electrophysiol* 2011;**4**:362–372.
25. Monovich L, Koch KA, Burgis R, Osimboni E, Mann T, Wall D, Gao J, Feng Y, Vega RB, Turner BA, Hood DB, Law A, Papst PJ, Koditek D, Chapo JA, Reid BG, Melvin LS, Pagratis NC, McKinsey TA. Suppression of HDAC nuclear export and cardiomyocyte hypertrophy by novel irreversible inhibitors of CRM1. *Biochim Biophys Acta* 2009;**1789**:422–431.
26. del Monte F, O'Gara P, Poole-Wilson PA, Yacoub M, Harding SE. Cell geometry and contractile abnormalities of myocytes from failing human left ventricle. *Cardiovasc Res* 1995;**30**:281–290.
27. Nikolaev VO, Moshkov A, Lyon AR, Miragoli M, Novak P, Paur H, Lohse MJ, Korchev YE, Harding SE, Gorelik J. Beta2-adrenergic receptor redistribution in heart failure changes cAMP compartmentation. *Science* 2010;**327**:1653–1657.
28. Simpson P. Stimulation of hypertrophy of cultured neonatal rat heart cells through an alpha 1-adrenergic receptor and induction of beating through an alpha 1- and beta 1-adrenergic receptor interaction. *Circ Res* 1985;**56**:884–894.
29. Behr TM, Nerurkar SS, Nelson AH, Coatney RW, Woods TN, Sulpizio A, Chandra S, Brooks DP, Kumar S, Lee JC, Ohlstein EH, Angermann CE, Adams JL, Sisko J, Sackner-Bernstein JD, Willette RN. Hypertensive end-organ damage and premature mortality are p38 mitogen-activated protein kinase-dependent in a rat model of cardiac hypertrophy and dysfunction. *Circulation* 2001;**104**:1292–1298.
30. Dash R, Schmidt AG, Pathak A, Gerst MJ, Biniakiewicz D, Kadambi VJ, Hoit BD, Abraham WT, Kranias EG. Differential regulation of p38 mitogen-activated protein kinase mediates gender-dependent catecholamine-induced hypertrophy. *Cardiovasc Res* 2003;**57**:704–714.
31. Kyoi S, Otani H, Matsuhisa S, Akita Y, Tatsumi K, Enoki C, Fujiwara H, Imamura H, Kamihata H, Iwasaka T. Opposing effect of p38 MAP kinase and JNK inhibitors on the development of heart failure in the cardiomyopathic hamster. *Cardiovasc Res* 2006;**69**:888–898.
32. Liu YH, Wang D, Rhaleb NE, Yang XP, Xu J, Sankey SS, Rudolph AE, Carretero OA. Inhibition of p38 mitogen-activated protein kinase protects the heart against cardiac remodeling in mice with heart failure resulting from myocardial infarction. *J Card Fail* 2005; **11**:74–81.
33. Wenzel S, Muller C, Piper HM, Schluter KD. p38 MAP-kinase in cultured adult rat ventricular cardiomyocytes: expression and involvement in hypertrophic signalling. *Eur J Heart Fail* 2005;**7**:453–460.
34. Petrich BG, Wang Y. Stress-activated MAP kinases in cardiac remodeling and heart failure: new insights from transgenic studies. *Trends Cardiovasc Med* 2004;**14**:50–55.

35. Wenzel S, Abdallah Y, Helmig S, Schafer C, Piper HM, Schluter KD. Contribution of PI 3-kinase isoforms to angiotensin II- and alpha-adrenoceptor-mediated signalling pathways in cardiomyocytes. *Cardiovasc Res* 2006;**71**:352–362.
36. Czubryt MP, Austria JA, Pierce GN. Hydrogen peroxide inhibition of nuclear protein import is mediated by the mitogen-activated protein kinase, ERK2. *J Cell Biol* 2000; **148**:7–16.
37. Cao DJ, Wang ZV, Battiprolu PK, Jiang N, Morales CR, Kong Y, Rothermel BA, Gillette TG, Hill JA. Histone deacetylase (HDAC) inhibitors attenuate cardiac hypertrophy by suppressing autophagy. *Proc Natl Acad Sci USA* 2011;**108**:4123–4128.s
38. Harrison BC, Roberts CR, Hood DB, Sweeney M, Gould JM, Bush EW, McKinsey TA. The CRM1 nuclear export receptor controls pathological cardiac gene expression. *Mol Cell Biol* 2004; **24**:10636–10649.